# Accurate time dependent wave packet calculations for the N + OH reaction

Niyazi Bulut, Octavio Roncero, Mohamed Jorfi, and Pascal Honvault

Citation: J. Chem. Phys. **135**, 104307 (2011); doi: 10.1063/1.3633240
View online: http://dx.doi.org/10.1063/1.3633240
View Table of Contents: http://jcp.aip.org/resource/1/JCPSA6/v135/i10
Published by the American Institute of Physics.

# Accurate time dependent wave packet calculations for the N + OH reaction

Niyazi Bulut,[1,a)] Octavio Roncero,[2] Mohamed Jorfi,[3] and Pascal Honvault[4]
[1]*Firat University, Department of Physics, 23169 Elazig, Turkey*
[2]*Instituto de Física Fundamental, C.S.I.C. Serrano 123, 28006 Madrid, Spain*
[3]*LOMC - Université du Havre, 25 Rue Philippe Lebon, BP 540 - 76 058 Le Havre Cedex, France*
[4]*Laboratoire Interdisciplinaire Carnot de Bourgogne, UMR CNRS 5209, Université de Bourgogne, 21078 Dijon Cedex, France*

(Received 24 June 2011; accepted 16 August 2011; published online 9 September 2011)

We present accurate quantum calculations of state-to-state cross sections for the N + OH → NO + H reaction performed on the ground $^3A''$ global adiabatic potential energy surface of Guadagnini *et al.* [J. Chem. Phys. **102**, 774 (1995)]. The OH reagent is initially considered in the rovibrational state $v = 0$, $j = 0$ and wave packet calculations have been performed for selected total angular momentum, $J = 0$, 10, 20, 30, 40,...,120. Converged integral state-to-state cross sections are obtained up to a collision energy of 0.5 eV, considering a maximum number of eight helicity components, $\Omega = 0,...,7$. Reaction probabilities for $J = 0$ obtained as a function of collision energy, using the wave packet method, are compared with the recently published time-independent quantum mechanical one. Total reaction cross sections, state-specific rate constants, opacity functions, and product state-resolved integral cross-sections have been obtained by means of the wave packet method for several collision energies and compared with recent quasi-classical trajectory results obtained with the same potential energy surface. The rate constant for OH($v = 0$, $j = 0$) is in good agreement with the previous theoretical values, but in disagreement with the experimental data, except at 300 K.  [doi:10.1063/1.3633240]

## I. INTRODUCTION

The heavy-heavy-light (HHL) type reaction

$$N(^4S) + OH(^2\Pi) \rightarrow H(^2S) + NO(^2\Pi),$$
$$\Delta H^\circ = -46\,\text{kcal/mol} \quad (1)$$

is a prototype reaction between open-shell atom N, and hydroxyl radical OH, and plays an important role in the atmospheric chemistry of the Earth[1] and in astrochemistry.[2] It belongs to the class of radical-radical reaction, such as the C + OH (Refs. 3–6) and F + OH (Refs. 7–10) reactions both studied extensively theoretically on several electronic states correlating to the ground state of reactants. From the dynamical point of view, such systems with two heavy atoms usually involve potential energy surfaces which present deep potential wells and many channels have to be considered to get converged results.

The title reaction has been the subject of many theoretical[11–15] and experimental[16–19] works. Experimentalists, in general, have focused on the determination of thermal rate constants. Smith and co-workers[18,19] have obtained experimental rate constants down to 103 K using discharge-flow and flash photolysis techniques. They found that the rate constant increases as the temperature decreases, and the measured thermal rate constants were found to present a nonlinear Arrhenius behavior over the temperature range studied. Experimental vibrational distribution of the NO product has also been measured by laser-induced fluorescence spectroscopy,[18] and it was found somewhat hotter than expected using statistical models.

The first *ab initio* potential energy surface (PES) for the N + OH → NO + H reaction was built by Guadagnini *et al.*[20] This PES was based on complete active space self-consistent field (CASSCF)/internally contracted configuration interaction calculation and fitting of the 800 *ab initio* points obtained at the (multireference configuration interaction) MRCI/cc-pVTZ level. It was found that the N + OH → NO + H reaction has no barrier relative to the entrance channel and a double well along the reaction path, corresponding to HON and HNO configuration geometries. It has been shown that, initially, this reaction leads to the formation of a HON complex,[20] bound by 3.07 eV relative to the entrance channel. Because of the open shell character of the reactants, there are several electronic states correlating to the N($^4S$) + OH($^2\Pi$) entrance channel, namely, $^3A'$, $^3A''$, $^5A'$, and $^5A''$. Only the triplet surfaces can correlate to the ground state of the H($^2S$) + NO ($^2\Pi$) products. The $^3A'$ surface is known to be strongly repulsive in the product channel.[22] Therefore, the $^3A''$ surface is the only surface joining the ground states of reagents and products.

The first dynamical calculations on this PES were carried out by using quasi-classical trajectory (QCT) (Ref. 21) and wave packet (WP) methods.[23] It was found that in the QCT calculations including the electronic degeneracy factor related to the fine structure of reactants, the total rate constant in the studied range of temperature was nearly independent of temperature. Also the rate constants were calculated using WP methods and compared with the QCT results in the same range of temperature. It was found that the WP rate constants

a)Author to whom correspondence should be addressed. Electronic mail: bulut_niyazi@yahoo.com.

 

were in quantitative disagreement with the previous QCT results for temperature below 500 K.

More detailed WP results were reported more recently on the N + OH reaction by Ge *et al.*[11] In their work, total reaction probabilities at selected total angular momentum, $J$, and state-selected rate constant at a range of 5 K–500 K temperature were calculated. The resonance structures present on the calculated reaction probabilities were found to be dependent on the total angular momentum, $J$, becoming broader and less intense as $J$ gets larger. Negative dependence on the temperature was observed on the calculated rates by using close-coupling scheme and it was found that this behavior is in good agreement with the previously obtained experimental results.[16]

Employing the same PES, Jorfi *et al.*[12] performed new QCT calculations to obtain the influence of reagent's rotational excitation on the dynamics of the N + OH reaction. They have found that the rotational excitation of the hydroxyl radical has significant effects on the excitation functions and rate constants. Following this work, Jorfi *et al.*[13] used a time-independent quantum mechanical (TIQM) method based on hyperspherical coordinates to obtain quantities at the state-to-state level. A detailed QCT study[14] reported the differential cross sections (DCS) and product energy distributions on the same PES. The TIQM state-to-state reaction probabilities were obtained for a total angular momentum $J = 0$ for collision energy up to 0.7 eV. The TIQM vibrational and rotational product distributions were also reported.[13] The effect of the collision energy on the reactivity was investigated in detail. The QCT total DCS presents pronounced forward and backward peaks and this behavior was observed in all the QCT vibrational state-resolved DCSs.

Very recently, a new global *ab initio* potential energy surface for the lowest triplet state of N + OH system has been published,[15] designed to characterize the N + OH → NO + H reaction. This PES was based on MRCI + Q calculations with a large (aug-cc-pV5Z) basis set. The details of the PES are given in Ref. 15. Dynamical calculations on this new PES have also been done by using a WP method. In those calculations, the main objective was to compute the total reaction probabilities as a function of collision energy without resolving for the final quantum states of the products. Initial state probabilities, up to $J = 105$, were calculated as a function of energy and then used to get integral cross sections (ICS). The reported WP rate constant is in reasonable agreement with the QCT prediction,[12] but smaller than the experimental ones.

The aim of the present work is to study the state-to-state dynamics of the N + OH→ NO + H reaction at collision energies below 0.5 eV on the PES built by Guadagnini *et al.*[20] Using an accurate quantum WP method, total and product vibrational state-resolved ICSs have been obtained and compared with QCT results. For $J = 0$, the state-to-state reaction probabilities are also compared with the TIQM calculations. Accurate quantum mechanical state-to-state ICSs for the title reaction are reported for the first time. Furthermore, the state-specific WP rate constant for OH($v = 0$, $j = 0$) is determined and compared with the QCT and experimental results.

TABLE I. Parameters used in the wave packet calculations (all distances are given in angstroms units unless otherwise specified).

| | |
|---|---|
| Reactant scattering coordinate range: | $R_{\min} = 0.001$; $R_{\max} = 19.0$ |
| Number of grid points in R: | 720 |
| Diatomic coordinate range: | $r_{\min} = 0.1$; $r_{\max} = 19.0$ |
| Number of grid points in r : | 240 |
| Number of angular basis functions : | 72 |
| Center of initial wave packet : | $R_0 = 7.0$ |
| Initial translational kinetic energy/eV : | $E_c = 0.285$ |
| Analysis point: | =4.0 |
| Number of Chebyshev iterations: | 80 000 |

## II. METHOD

The dynamics of H + HL → HH + L reactions have been extensively studied in the literature.[3–6,24–26] The N + OH($v = 0$, $j = 0$) → NO + H reaction is a prototype of H + HL reactions and has been studied using a WP method and QCT approach described in detail in the literature.[11–15] The propagation of the wave packet may be carried out in reactant or product Jacobi coordinates. For this kind of systems, it has been demonstrated that it is more efficient to use reactant Jacobi coordinates.[28] The present state-to-state reaction probabilities are calculated using a wave packet method, with the code MADWAVE3 recently reported by Zanchet *et al.*[29] The MADWAVE3 codes based on wave packet method have been well documented in the literature[9,29] and only the details relevant to the present work will be given here. In the present calculations, the initial wave packet is located in the asymptotic reactant channel where there is no influence of the interaction potential, and the propagation grid scheme is defined using the same reactant Jacobi coordinates. In order to calculate the reaction probabilities, it is necessary to integrate the initial wave packet flowing into the possible channels. The properties of initial wave packet and the grid parameters are given in Table I, which were converged for $J = 0$ and then used for the rest of $J$'s calculated.

The calculation of the ICSs as a function of collision energy for each rovibrational state $v$, $j$ of the reagent molecule, $\sigma_{v,j}(E_c)$ requires summing up the contributions from all possible values of the total angular momentum $J$,

$$\sigma_{vj}(E_c) = \frac{\pi}{k^2}\frac{1}{2j+1}\sum_{J=0}^{J_{\max}}(2J+1)P_{vj}^{J}(E_c), \qquad (2)$$

where $k^2 = 2\mu_r E_c/\hbar^2$, and $P_{v,j}^{J}(E_c)$ is the reaction probability from the initial rovibrational state $v$, $j$ summed over all final states as a function of collision energy, $E_c$, at a total angular momentum $J$.

The coupled-channel (CC) calculations have been performed for selected total angular momentum, $J = 0$, 10, 20, 30, 40,...,120, needed to calculate the cross sections up to 0.5 eV. These calculations included up to eight helicity components, $\Omega = 0,...,7$. Intermediate total angular momenta or partial waves are obtained by an interpolation procedure based on the $J$-shifting approach.[32] With this approach, the reaction probability for a given $J$ value, $J \in [J1, J2]$,

is obtained as

$$P_J(E) = \frac{J - J_1}{J_2 - J1} P_{J_1}(E - B[J(J+1) - J_1(J_1+1)]) + \frac{J_2 - J}{J_2 - J1} P_{J_2}(E + B[J_2(J_2+1) - J(J+1)]), \quad (3)$$

where $B = \hbar^2/2\mu R^2$ rotational constant has a value of 0.2 meV. Thus, the total ICSs are obtained by using Eq. (2).

The $v$, $j$ initial state-selected rate constant is calculated by averaging the corresponding ICS $\sigma_{vj}(E_c)$ over translational energy as

$$k_{vj}(T) = \frac{3}{Q_{el}} \left(\frac{8}{\pi \mu_r (k_B T)^3}\right)^{1/2} \times \int_0^\infty E_c \, \sigma_{vj}(E_c) e^{-E_c/k_B T} \, dE_c, \quad (4)$$

where $k_B$ is the Boltzmann constant, 3 is the degeneracy of the $^3A''$ PES, $E_c$ is the translational energy, and $Q_{el}$ is the electronic partition function. For the title reaction, the electronic partition function is given by[12]

$$Q_{el} = 4 \times [2 + 2\exp(-205/T)]. \quad (5)$$

## III. RESULTS AND DISCUSSION

### A. Reaction probabilities

Figure 1 displays the exact total N + OH($v = 0$, $j = 0$) reaction probability as a function of collision energy calculated using the WP method for $J = 0$. The WP probability shows a sharp rise at nearly zero energy and after that a sequence of narrow peaks or resonances. These quantum resonances are associated with a long-lived intermediate complex formed in the deep HON and HNO wells of the PES which supports many quasibound states. The reaction probability calculated, using a TIQM method,[13] is also plotted in Fig. 1. The overall behavior of the results obtained with the two methods is rather similar.

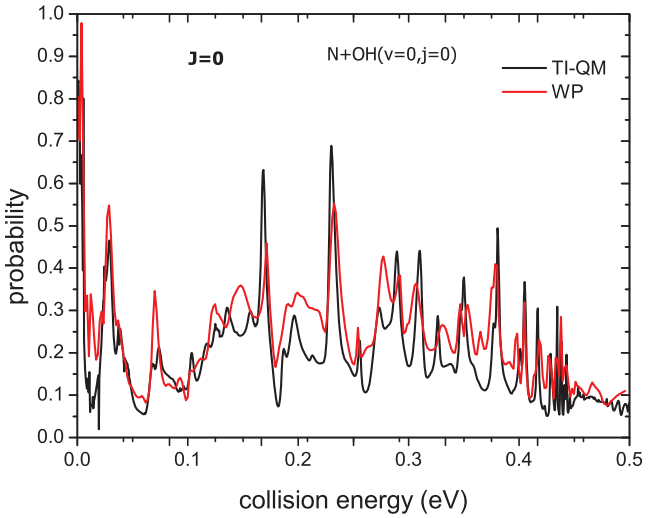


FIG. 1. TIQM and WP total reaction probabilities as a function of collision energy for total angular momentum $J = 0$ calculated for the N + OH($v = 0$, $j = 0$)→ NO + H reaction.

In the presence of deep wells, the reaction probabilities typically show many narrow oscillations associated with resonances. These resonances correspond to very excited quasibound states, which depending on the system and energy range, may correspond to an ordering quantum number of several hundreds or even thousands. In order to accurately account for the nodal structure of such quasibound states, one would need to include possibly thousand of points in all degrees of freedom. Due to the difficulty to get convergence, any small difference between two methods would give different results. The convergence problem is larger for the WP methods, but is also present in TIQM methods. In addition, different sets of coordinates (Jacobi/hyperspherical) also introduce differences between the results when these convergence problems are present. This situation makes that the position of individual peaks obtained using two different methods/coordinates are slightly shifted one with respect to each other, with a different shift for each resonance. However, the background envelope of the reaction probability is typically in good agreement, as it happens in this case. This situation has already been observed for other reactions with deep insertion wells, such as $H_3^+$ system.[30,31] This may explain the quantitative disagreement between the two quantum results. It is worthwhile to note that the present WP results are very similar to those reported by Ge *et al.*[11] at $J = 0$ using the same coordinates and PES.

The vibrational state resolved reaction probabilities at total angular momentum $J = 0$ are compared with TIQM results,[13] in Fig. 2. The agreement between the two sets of results is rather good, both showing the same order of magnitude and behavior for all the $v'$. For a more detailed comparison, in Fig. 3, the WP and TIQM vibrational distributions at $J = 0$ for the N + OH($v = 0$, $j = 0$) → NO($v'$) + H reaction are compared at two selected collision energies, 0.05 and 0.1 eV. The WP and TIQM results for both 0.05 eV and 0.1 eV collision energies are again in a fairly good agreement. In both cases, the reaction probability decreases as $v'$ increases, but showing some weak oscillations. The position of these oscillations is approximately the same in WP and TIQM results, but the amplitudes present some differences.

The reaction is very exothermic, by ≈ 2.11 eV, giving rise to many open channels in the NO + H products channel, up to $v' = 13$ for the energies considered, including many rotational states due to the small rotational constant of NO, ≈ 0.2 meV. The final vibrational probability of products, essentially decreasing with $v'$ seems to indicate that the situation is statistical. This may also be justified by the presence of many peaks in the reaction probabilities, associated with quasibound states originated by either of the two deep wells of the PES, corresponding to HON and HNO isomers. These wells are rather deep, ≈ 4 eV below the OH + N entrance channel, but the resonances are located more than 2 eV above the first dissociation threshold, NO($v' = 0$) + H, what makes that the resonances are relatively narrow, of the order of 5–10 meV, with lifetimes of the order 1–50 fs.

Following these arguments, one may think that reaction follows a typical statistical mechanism, in which first a

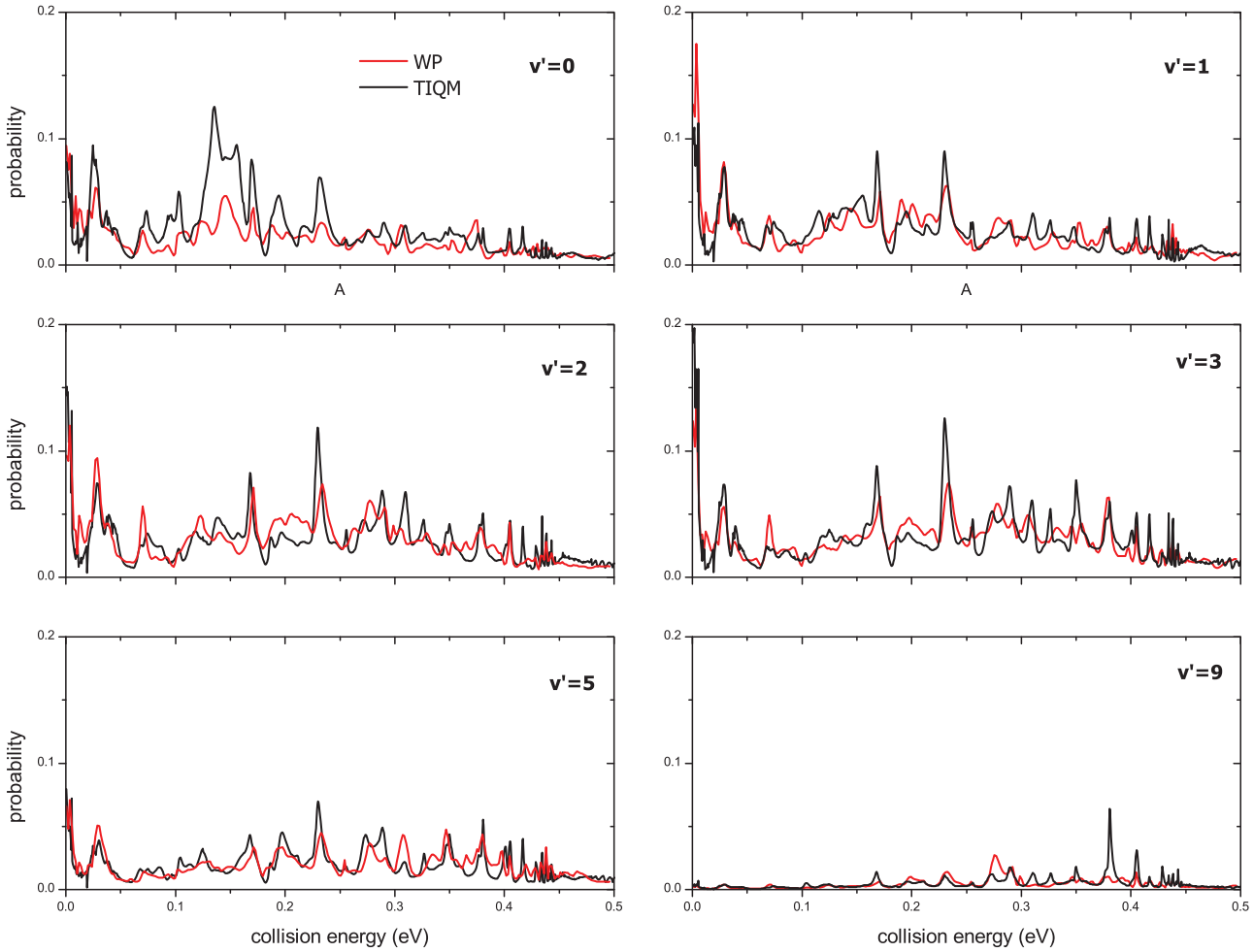


FIG. 2. TIQM and WP vibrational state resolved probabilities as a function of collision energy for the N + OH($v = 0$, $j = 0$)→ H + NO($v'$) reaction.

complex is formed, and then it fragments through the different available open channels with the same probability.[33–35] If this is so, the total reaction probability, in Fig. 1, would have been close to one, since there are huge amount of open channels in the product channels, in contrast to the few channels of OH + N reactants. However, the reaction probability is of the order of 0.2 in average, except at some of the resonances where it may increase more. This may indicate that the formation of the complex is not direct, but is preceded by some limiting step, which reduce the probability of complex forming. The PES landscape is complicated, showing two minima, corresponding to two linear isomers, HNO and NOH, with a barrier among them. The NO + H product channel is directly connected to the HNO well. The resonances of NOH well may dissociate directly following another path in the PES or by isomerizing first to the HNO well. Thus, the number of competing processes complicates the analysis but already demonstrate the complexity of this otherwise apparent simple reaction. A more detailed study through QCT calculations may be of help.

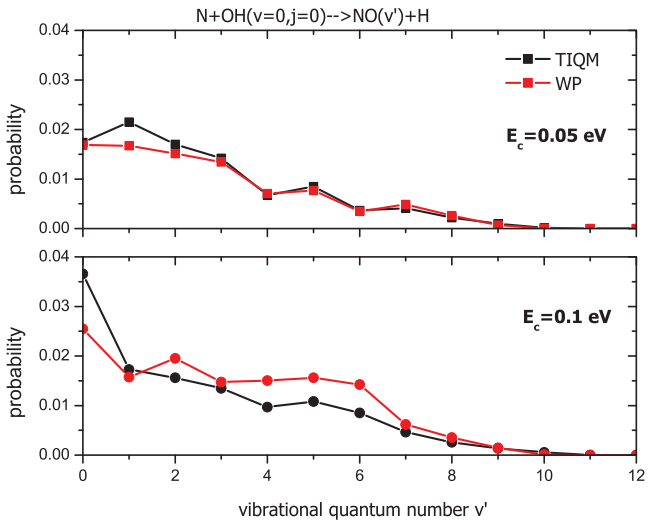


FIG. 3. TIQM and WP product vibrational distributions as selected (0.05, 0.1 eV) collision energies.

Total reaction probabilities for selected values of $J$ are shown in Fig. 4. As $J$ increases the reaction energy threshold shifts towards higher collision energy values due to the centrifugal barrier. The highest $J$ calculated in this work, using the WP method, has been $J = 110$. In all cases, there are narrow peaks associated with resonances, indicating that, even for high $J$, the collision is dominated by long-lived resonances associated with the deep HON well. At resonances, the system is long time at short distances, where

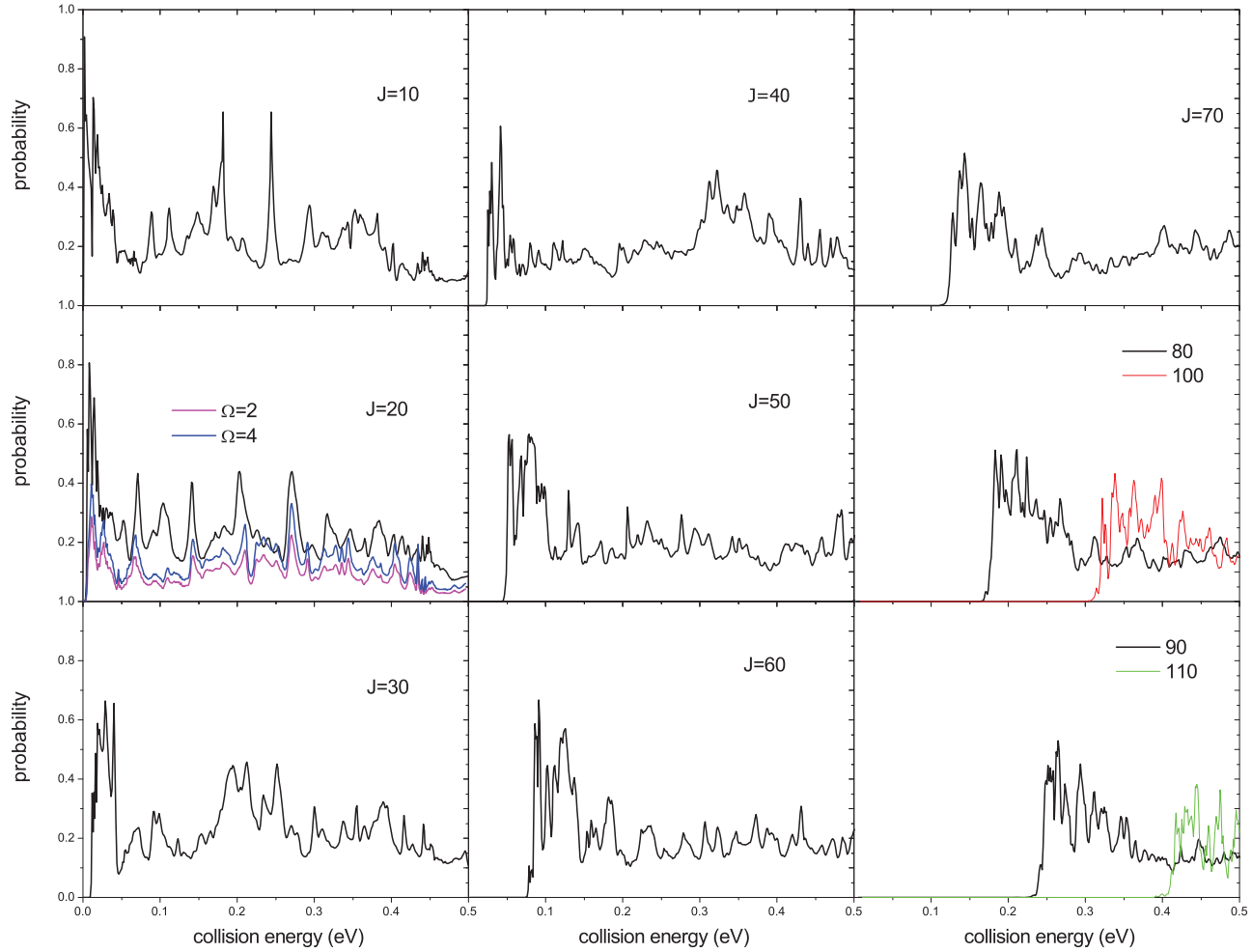


FIG. 4. WP total reaction probabilities as a function of collision energy for the N + OH($v = 0$, $j = 0$)→ H + NO reaction at selected $J$ values.

the Coriolis coupling is higher. This is why, the centrifugal sudden approach (CSA), in just one helicity component Ω is introduced in the calculation, leads to bad results. The reason is that when considering all Ω's, the number of rotational sublevels increases and equivalently the number of resonances. These resonances are coupled through Coriolis couplings so they share their intensity and give rise to broader and less structured features in the reaction probability. In Fig. 4, the CS results are compared with CC results with increasing the number of Ω's for the case of $J = 20$. The fast convergence with the increase of helicity functions indicates that the use of reactant Jacobi coordinates, as expected for the mass combination,[28] The use of product Jacobi coordinates would require the inclusion of a higher number of Ω's, making the calculation of state-to-state probabilities very difficult.

Figure 5 shows the total reaction probability as a function of $J$ (i.e., opacity function), calculated at four specific collision energies by means of the WP method and QCT approach. Both the WP and QCT results exhibit a very similar behavior in terms of $J$, specially at the higher energy considered of 0.5 eV. The main difference is the oscillations appearing in the WP calculations, due to resonances, which are not present in the QCT calculations. The QCT opacity is fairly constant as a function of $J$ and drops suddenly at high $J$. Although the QCT method does not produce a perfect quantitative description of the WP reaction probability, it is expected that it is going to work very well to reproduce quantities after the partial wave sum. This indicates that the QCT approach is going to be rather satisfactory for describing this reaction.

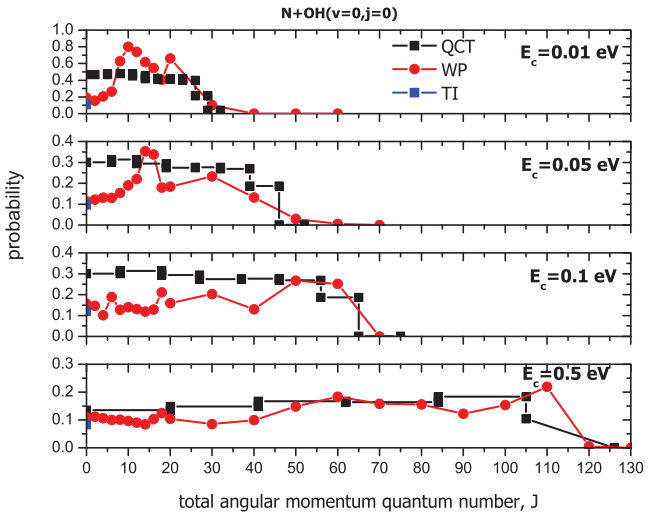


FIG. 5. Opacity function or reaction probability in terms of the total angular momentum $J$ calculated at some selected (0.01, 0.05, 0.1, 0.5 eV) collision energies obtained by the WP method and QCT approach.

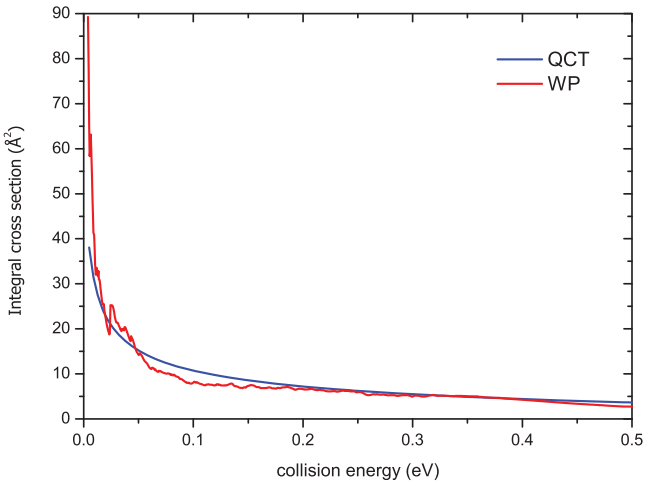


FIG. 6. QCT and WP integral cross sections as a function of collision energy for the N + OH($v = 0$, $j = 0$)→ H + NO.

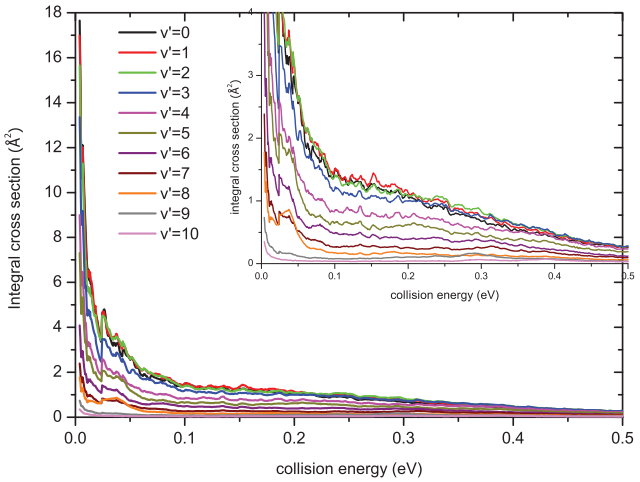


FIG. 7. WP product vibrational integral cross sections as a function of collision energy.

The nearly constant behavior of the QCT results are very similar to that expected from a statistical model. This indicates, again, that once the complex is formed, the reaction behaves statistically. In order to check this assumption, the two steps, formation of complex, and dissociation should be separated. The WP methods do not allow to perform such a calculation, since the WP spreads over all configuration space, and any separation would be rather artificial and with many problems. Another possibility would be the use of the statistical QCT method recently developed by Aoiz and co-workers.[37]

### B. Excitation functions and state-resolved integral cross sections

Figure 6 shows the WP and QCT ICSs as a function of collision energy (i.e., excitation functions) for the N + OH($v = 0$, $j = 0$) → NO + H reaction. The two ICSs decrease as collision energy increases without showing energy threshold. This behavior, which is characteristic of barrierless exothermic reactions, is similar, among others, to the radical-radical OH + O reaction, as recently reported by some groups.[38,39] The agreement between the WP and QCT excitation functions is quite good for the whole range of collision energies, except for low energies, below 0.05 eV, where the WP results are considerably larger than the QCT ones. The reason of the faster increase of the WP cross section is the resonances appearing near the threshold. Those resonances appear in both, the WP and TIQM calculations, showing a reasonably good quantitative agreement. However, since the WP methods have difficulties near the threshold, a denser grid in energy has been used and the reaction probability calculated for $J = 0$, 1, 2,..., 20, to avoid interpolation problems when using Eq. (3). After some checks, we conclude that for energies below 0.05 eV, the WP results are reliable, but the cross section can be slightly smaller, but higher than the QCT ones. It would be desirable at these low energies to perform TIQM calculations of the cross stection but in this reaction, because of the exothermicity and the deep wells, it is very hard.

The vibrationally resolved cross sections are shown in Fig. 7, as a function of collision energy, and for selected energies as a function of $v'$ are shown in Fig. 8 to compare with QCT results.[14] At 0.1 the results are also compared with the available experimental cross sections.[18] The cross section decreases as a function of energy, for all the $v'$ considered, showing some small structures, associated with resonances, and a sort of plateau between 0.1 and 0.25 eV. At energy zero, up to $v' = 9$ is open and at 0.5 eV the channel $v' = 12$ is already open. These levels are formed with very low probability in the whole energy range considered just because they support fewer rotational level than the lower vibrational states. The cross sections obtained for $2 < v' < 9$ do not cross all showing the same decreasing behavior. In the case of the lower $v'$ = 0, 1, and 2, they present very similar cross sections, and they cross at some energies.

This is more clearly shown in Fig. 8 at three selected collision energies, 0.05, 0.1, and 0.5 eV. At 0.05 eV the WP cross section shows a completely decreasing behavior, as one expects using pure statistical arguments. However, for 0.1 eV,

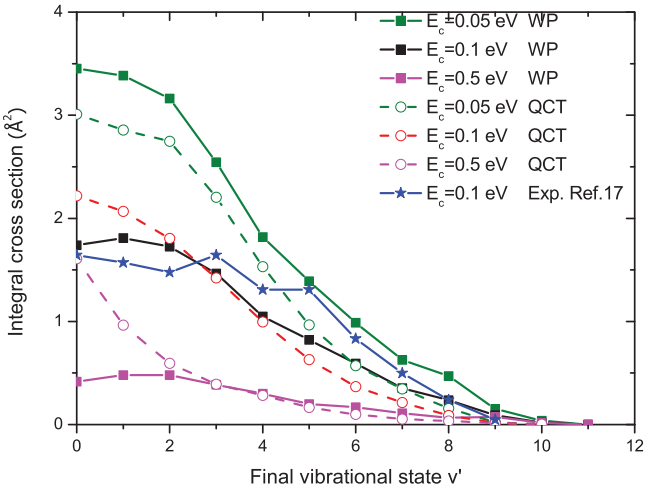


FIG. 8. WP and QCT product vibrational distributions for the N + OH($v = 0$, $j = 0$) → H + NO($v'$) reaction at 0.05 and 0.1 eV collision energies.

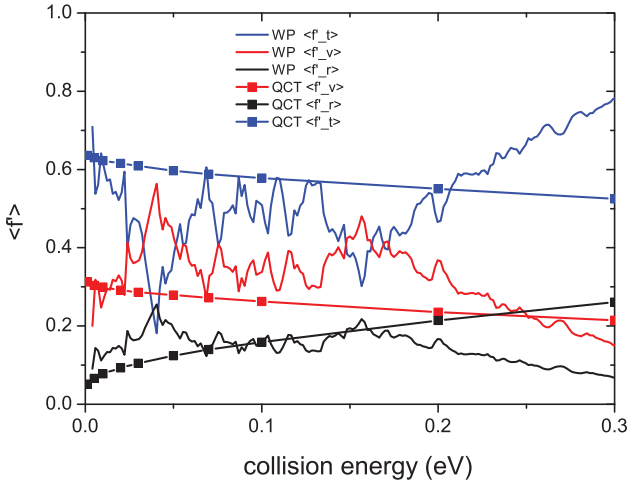


FIG. 9. Dependence on the collision energy of the average fraction of the total available energy in the product motion for rotation, vibration, and translation($< f_r >, < f_v >, < f_t >$) for the N + OH($v = 0, j = 0$) →NO + H reaction.

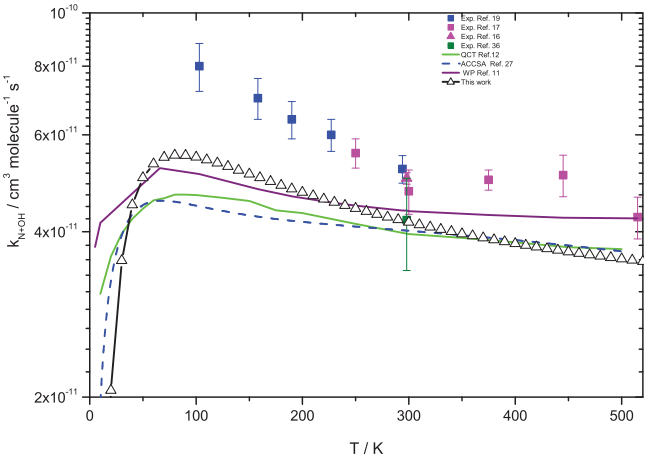


FIG. 10. Comparisons between calculated and experimental rate constants as a function of temperature.

there is a maximum for $v' = 1$, which seems to shift to $v' = 2$ at 0.5 eV. This slight vibrational inversion is not statistical. At higher energies, resonances become broader, and directlike mechanisms can start competing with the statistical mechanism mentioned. This could explain this small vibrational inversion. Notice that the experimental results for 0.1 eV show a maximum at $v' = 3$, and a structure similar to a plateau up to $v' = 3$ or 4, followed by a fast decreased for higher $v'$. This result is in good agreement with the WP results; the QCT cross sections, however, decrease with $v'$, and at low energies when $v' = 0$ and 1 become nearly equal. Thus, these features, discussed for low $v'$, are described differently by the QCT and WP methods, but the overall behavior is rather good.

Average fraction of the total available energy in the product motion for rotation, $< f'_r >$, vibration, $< f'_v >$, and translation, $< f'_t >$, is shown in Fig. 9 as a function of collision energy. The quantum and classical[12] results are relatively similar in magnitude, but while QCT results present a monotonous behavior with energy. The WP results show structures, which are again associated with resonances. At high energies, The QCT and WP rotational and translational fractions present a different behavior: while WP $f_r$ decreases, QCT $f_r$ increases, and the $f_t$ presents the opposite behavior. At low energies, the agreement between QCT and WP is better, and all fractions are more similar. This may indicate that in this regime the dynamics is more statistical. At higher energies, however, the translational energy fraction is considerably larger than the others, probably indicating that the dynamics becomes more direct, without spending so much time in the well. The QCT results are lower than the WP $f_t$, probably because the trajectories still keep trapped in the potential wells, overestimating the indirect statistical reaction mechanism.

### C. Rate constant

The initial state-selected rate constant for the OH($v = 0, j = 0$) rovibrational state has been calculated up to 500 K using the cross section, in Eq. (4), and it is shown in Fig. 10. In the figure it is compared with previous results, both theoretical and experimental. The present results are close, but not the same to those previously reported by Ref. 11, obtained also with the WP calculations. These are attributed to the different number of Ω functions in the two sets of calculations: here, we use eight helicities, while in Ref. 11 only four are included. In the panel of $J = 20$ of Fig. 4, the reaction probability obtained using four helicities is lower than in the case of eight, what explains the difference.

Also, the present WP results are higher than the QCT results of Ref. 13 and the adiabatic capture centrifugal sudden approximation method of Ref. 27. This is due to the resonances appearing at the threshold, which makes that the total cross section increases more rapidly as the collision energy goes to zero, as explained above.

The comparison at T = 298 K, the WP rate constant ($4.17\ 10^{-11}$ cm$^3$ molecule$^{-1}$ s$^{-1}$) is in excellent agreement with the experimental value of $4.2\ 10^{-11}$ cm$^3$ molecule$^{-1}$ s$^{-1}$ of Brune *et al.*[36] However, the present WP rate constant, such as all the theoretical rate constants, is in disagreement with the other experimental results, even if the dependence on temperature is well reproduced by the WP result. The present WP rate constant is also in good agreement with the very recently published WP rate constant computed using a new PES.[15] Apart from deficiencies in the PES, dealing with open shell systems, the inclusion of other electronic states correlating to the OH($^2\Pi$) + N($^4S$) asymptote could also yield to an increase of the rate constants.[9]

## IV. CONCLUSIONS

In this study, the WP calculations using the MADWAVE3 code for the N + OH($v = 0, j = 0$) → NO + H reaction have been performed for total angular momentum $J \geq 0$, using an *ab initio* PES built by Guadagnini *et al.*[20] State-to-state ICSs have been obtained for the first time using an accurate quantum mechanical method. The WP results have been compared with QCT calculations. The total ICS has been computed and the calculated WP and QCT excitation functions

decrease with increasing collision energy, as expected for an exothermic barrierless reaction. An overall good agreement between the WP and QCT reaction probabilities and ICSs (vibrational distribution) has been found. Initial ($v = 0$, $j = 0$) state-selected WP rate constant has been calculated using the corresponding excitation function. Again, the WP and QCT rate constants are in a fairly good agreement. However, a disagreement is still found between the theoretical rate constants (this work and other QCT and WP studies) and the experimental results. New experiments are therefore needed, especially below 300 K.

## ACKNOWLEDGMENTS

Partial financial support from the Scientific and Technological Research Council of TURKEY (TUBITAK) (Project No. TBAG-109T447) and Firat University Scientific Research Projects Unit (FUBAP-1775) is gratefully acknowledged. Wave packet computations have also been done on the High Performance and Grid Computing Center (TR-Grid) machine at ULAKBIM/TURKEY. O.R. acknowledges the financial support of Ministerio de Ciencia e Innovación (Spain) under Grant No. CSD2009-00038.

[1] R. P. Wayne, *Chemistry of Atmospheres*, 3rd ed. (Oxford University Press, New York, 2000).
[2] D. Carty, A. Goddard, S. P. K. Kohler, I. R. Sims, and I. W. M. Smith, J. Phys. Chem. A **110**, 3101 (2006).
[3] A. Zanchet, P. Halvick, J. C. Rayez, B. Bussery-Honvault, and P. Honvault, J. Chem. Phys. **126**, 184308 (2007).
[4] A. Zanchet, P. Halvick, B. Bussery-Honvault, and P. Honvault, J. Chem. Phys. **128**, 204301 (2008).
[5] N. Bulut, A. Zanchet, P. Honvault, B. Bussery-Honvault, and L. Bañares, J. Chem. Phys. **130**, 194303 (2009).
[6] M. Jorfi, P. Honvault, B. Bussery-Honvault, L. Bañares, and N. Bulut, Mol. Phys. **109**, 543 (2011).
[7] S. Gómez-Carrasco, L. González-Sánchez, A. Aguado, O. Roncero, J. M. Alvariño, M. L. Hernández, and M. Paniagua, J. Chem. Phys. **121**, 4605 (2004).
[8] S. Gómez-Carrasco, O. Roncero, L. González-Sánchez, M. L. Hernández, J. M. Alvariño, M. Paniagua, and A. Aguado, J. Chem. Phys. **123**, 114310 (2005).
[9] A. Zanchet, T. González-Lezana, A. Aguado, S. Gómez-Carrasco, and O. Roncero, J. Phys. Chem. A **114**, 9733 (2010).
[10] S. Gómez-Carrasco, A. Aguado, M. Paniagua, and O. Roncero, J. Chem. Phys. **125**, 164321 (2006).
[11] M. H. Ge, T. S. Chu, and K. L. Han, J. Theor. Comput. Chem. **7**, 607 (2008).
[12] M. Jorfi, P. Honvault, and P. Halvick, Chem. Phys. Lett. **471**, 65 (2009).
[13] M. Jorfi and P. Honvault, J. Phys. Chem. A **113**, 2316 (2009).
[14] M. Jorfi, P. Honvault, and P. Halvick, J. Chem. Phys. **131**, 094302 (2009).
[15] A. Li, C. Xie, D. Xie, and H. Guo, J. Chem. Phys. **134**, 194309 (2011).
[16] M. J. Howard and I. W. M. Smith, Chem. Phys. Lett. **69**, 40 (1980).
[17] M. J. Howard and I. W. M. Smith, J. Chem. Soc., Faraday Trans. **77**, 997 (1981).
[18] I. W. M. Smith, R. P. Tuckett, and C. J. Whitham, J. Chem. Phys. **98**, 6267 (1993).
[19] I. W. M. Smith and D. W. A. Stewart, J. Chem. Soc., Faraday Trans. **90**, 3221 (1994).
[20] R. Guadagnini, G. C. Schatz, and S. P. Walch, J. Chem. Phys. **102**, 774 (1995).
[21] R. Guadagnini, G. C. Schatz, and S. P. Walch, J. Chem. Phys. **102**, 784 (1995).
[22] M. C. Colton and G. C. Schatz, J. Chem. Phys. **83**, 3413 (1985).
[23] M. D. Chen, B. Y. Thang, K. L. Han, N. Q. Lou, and J. Z. H. Zhang, J. Chem. Phys. **118**, 6852 (2003).
[24] C. Xu, D. Xie, P. Honvault, S. Y. Lin, and H. Guo, J. Chem. Phys. **127**, 024304 (2007).
[25] S. Y. Lin, H. Guo, P. Honvault, C. Xu, and D. Xie, J. Chem. Phys. **128**, 014303 (2008).
[26] M. Jorfi, P. Honvault, P. Halvick, S. Y. Lin, and H. Guo, Chem. Phys., Lett. **462**, 53 (2008).
[27] D. Edvardsson, C. F. Williams, and D. C. Clary, Chem. Phys. Lett. **431**, 261 (2006).
[28] S. Gómez-Carrasco and O. Roncero, J. Chem. Phys. **125**, 054102 (2006).
[29] A. Zanchet, O. Roncero, T. González-Lezana, A. Rodriguez-López, A. Aguado, C. Sanz-Sanz, and S. Gómez-Carrasco, J. Phys. Chem. A **113**, 14488 (2009).
[30] T. González-Lezana, O. Roncero, P. Honvault, J.-M. Launay, N. Bulut, F. J. Aoiz, and L. Bañares, J. Chem. Phys. **125**, 094312 (2006).
[31] E. C. Novillo, T. González-Lezana, O. Roncero, P. Honvault, J.-M. Launay, N. Bulut, F. J. Aoiz, L. Bañares, A. Trottier, and E. Wrede, J. Chem. Phys. **128**, 014304 (2008).
[32] J. M. Bowman, Adv. Chem. Phys. **61**, 115 (1985).
[33] P. Pechukas, J. C. Light, and C. Rankin, J. Chem. Phys. **44**, 794 (1966).
[34] W. H. Miller, J. Chem. Phys. **52**, 543 (1970).
[35] E. J. Rackham, T. Gonzalez-Lezana, and D. E. Manolopoulos, J. Chem. Phys. **119**, 12895 (2003).
[36] W. H. Brune, J. J. Schwab, and J. G. Anderson, J. Phys. Chem. **87**, 4503 (1983).
[37] F. J. Aoiz, V. Saez Rabanos, T. Gonzalez-Lezana, and D. E. Manolopoulos, J. Chem. Phys. **126**, 161101 (2007).
[38] J. A. Kłos, F. Lique, M. H. Alexander, and P. J. Dagdigian, J. Chem. Phys. **129**, 064306 (2008).
[39] F. Lique, M. Jorfi, P. Honvault, P. Halvick, S. Y. Lin, H. Guo, D. Q. Xie, P. J. Dagdigian, J. Kłos, and M. H. Alexander J. Chem. Phys. **131**, 221104 (2009).